

APPLYING SATELLITE DATA FOR SHORELINE DETERMINATION IN TIDELAND AREAS

Lin T. H., Liu G. R., Chen A. J., and Kuo T. H.
Center for Space and Remote Sensing Research
National Central University, Chung-Li, Taiwan 320
E-mail:grliu@csrsr.ncu.edu.tw
Tel:(886)-3-4257232 Fax(886)-3-4255535
TAIWAN

KEY WORDS: Shoreline, SPOT, GPS

ABSTRACT: A simple model in determining the location of the shoreline on coastal zones is presented in this study. The main concept involves using the reflectance difference between the coastal land and its adjacent waters in the visible and near infrared spectral bands. Concurrent shoreline position measurements by GPS are also employed to construct and improve our approach. Three sets of SPOT HRV images, acquired in the clear sky condition, are used in this study. The results show that the gradient criteria of the shoreline position are stable, and can be used to find the shoreline easily in the clear sky cases. More examples should be investigated for constructing a database of gradient values for further applications around tideland areas in the future.

1. INTRODUCTION

Many of the global changes are caused by human activities, where particular emphasis is laid on coastal zones because roughly around 60% of the society's population live in this areas(Cracknell, 1999). The techniques of remote sensing can provide the capability for environmental monitoring in an economical and rapid way, either locally or globally. It plays an important role in keeping a constant eye on the frequent changes of our environment. In the investigation of tideland areas, the shoreline position serves as an important item(Chen and Rau, 1997). In the study of Chen and Rau(1997), the shoreline was extracted from pseudo color images by manual operation. Although a high level of accuracy can be obtained, the manual mode can not be applied when a serious blurring effect occurs (Sifakis et al., 1998). Based on the significant difference in reflectance of the VIS/NIR spectral bands between water and sand, the shoreline can be delineated more easily by a simpler gradient calculation which is called the "Gradient operator" in this study. The Gradient operator is compared with the Sobel operator, which is generally applied for change detection to test its practicality in the application of shoreline detection with remotely sensed data. The Gradient operator results show a small improvement over the Sobel operator, implying that the shoreline position can be detected by the Gradient operator. In order to obtain a more accurate detection, the GPS measurements of the shoreline

position which were concurrently made with the satellite observations were used as a reference in this study.

2. METHODOLOGY AND TEST

2.1 Characteristics of Objects' Reflectance

Due to the large difference in reflectance between water and sand in the VIS/NIR spectral bands, especially in the NIR(see also figure 1(a)), the shoreline position in the tideland areas can be extracted via this difference. The remotely sensed data acquired by SPOT HRV are used for the shoreline investigation in this study. Figure 1(b) shows the variance of reflectance between the SPOT HRV bands along the sample(row) direction across the Wai-San-Ting sand barrier in a clear sky condition. The X-axis and Y-axis represent the sample pixels and its digital counts of reflectance. The water and sand regions can be easily identified by the different value of digital counts, and the concurrent GPS measurements aid to detect the exact shoreline position which is represented by the symbol “+” in the figure. Once the characteristics (difference or gradient) of the shoreline have been obtained, the shoreline along the tideland area can be extracted by the remotely sensed data.

2.2 Operator Test

In order to detect the position of the shoreline, the Gradient operator is defined through equation (1) on a 3 x 3 window in this study.

$$GRA(i, j) = [\nabla_x^2 + \nabla_y^2]^{1/2} \quad (1)$$

$$\nabla_x(i, j) = DC(i, j-1) - DC(i, j+1)$$

$$\nabla_y(i, j) = DC(i-1, j) - DC(i+1, j)$$

The variables i and j are the line and column coordinates of the image, DC stands for digital counts, and the ∇_x and ∇_y mean the DC differences in the line and column direction. As mentioned above, the Gradient operator is compared with the Sobel operator which is generally applied for change detection and described by equation (2) in evaluating its accuracy and practicality.

$$BOL(i, j) = [\nabla_x^2 + \nabla_y^2]^{1/2} \quad (2)$$

$$\nabla_x(i, j) = DC(i-1, j+1) + 2DC(i, j+1) + DC(i+1, j+1) - DC(i-1, j-1) - 2DC(i, j-1) - DC(i+1, j-1)$$

$$\nabla_y(i, j) = DC(i-1, j-1) + 2DC(i-1, j) + DC(i-1, j+1) - DC(i+1, j-1) - 2DC(i+1, j) - DC(i+1, j+1)$$

$$- 2DC(i + 1, j) - DC(i + 1, j + 1)$$

Both the Gradient and Sobel operators are applied to the area around an image of Taichung port, which was acquired by SPOT HRV on January 30, 1996 (figure 2(a)). The results show a similar result in the shoreline detection on the test area by both operators (see also figure 2(b)). On the other hand, from the discontinuities of both detected shorelines, the Gradient operator seemed to be more practical than the Sobel operator. They were compared with concurrent GPS measurements, where the $GRA(i,j)$ values of the shoreline position were 2.2 in the SPOT HRV/XS1 and 3.4 in the XS3 in the clear sky case.

3. RESULTS

Besides the case in article 2, the other two case studies were investigated with the ground truth of shoreline in this paper (shown in table 1).

3.1 Case1 : Wai-San-Ting Sand Barrier

The study area is shown in figure 3(a) during a clear sky, and the results of the shoreline detected by the Gradient operator with GPS data is illuminated in figure 3(b). The red and green shorelines obtained by the XS1 and XS3 data respectively seems to be very consistent, and accurately pinpoints the shoreline position when compared with the GPS measurements (cyan points). On the other hand, the Gradient operator fails when spindrifts occur (see also figure 3(b)).

3.2 Case 2 : Taichung Port

The study area is shown in figure 4(a) during a clear sky condition, and the results of the shoreline detected by the Gradient operator is illuminated in figure 4(b). Contrary to case 1, the red and green shorelines does not seem to be consistent. Because of having a stronger transmittance through water than the XS3, the XS1 is affected more by the substrate. However, the shoreline detection could still work with the XS3 data but failed with the XS1 data around the river outlet area.

The satisfactory results of the 2 cases above illuminate that it is very practical to detect the shoreline position through application of the Gradient operator to the SPOT HRV data, especially with the XS3 data. And the gradient values of the shoreline detection are very similar in all case studies (table 2).

4. DISCUSSIONS

A simple and effective method for shoreline detection in tideland areas with SPOT HRV data is represented in this study. The results from 3 case studies show that the SPOT HRV/XS3 data would be a wise choice for shoreline extraction in a either a clear or hazy sky. The stable gradient values can also

be used for the extraction of shorelines with SPOT HRV/XS3 data in the clear sky cases. However, more examples should be collected to determine the characteristics of shorelines, and construct a database of gradient values for more applications in tideland areas.

5. REFERENCES

Chen L. C., and J. Y. Rau, 1998. Detection of shoreline change for tideland area using multi-temporal satellite images. *INT. J. Remote Sensing*, Vol. 19, No. 17, 3383-3397.

Cracknell A. P., 1999. Remote sensing techniques in estuaries and coastal zones-an update. *INT. J. Remote Sensing*, Vol. 19, No. 3, 485-496.

Richards J. A., 1986. Remote sensing digital image analysis. Springer-Verlag Berlin Heidelberg, Germany, pp. 281.

Sifakis N. I., Soulakellis N. A., and Paronis D. K., 1998. Quantitative mapping of air pollution density using earth observations: A new processing method and application to an urban area. *INT. j. Remote Sensing*, Vol. 19, No. 17, 3289-3300.

Table 1. The case studies of SPOT HRV imagery in this study.

Satellite	Date	Area	Weather condition
SPOT 2	1998/11/12	Wai-San-Ting sand barrier	Clear
SPOT 1	1999/04/29	Taichung port	Clear
SPOT 1	1997/11/25	Guanyin beach	Heavy haze

Table 2. The gradient values of the shoreline position of all cases used in this study.

Date	Area	Weather condition	Gradient value of shoreline position	
			XS1	XS3
1996/01/30	Taichung port	Clear	2.2	3.4
1998/11/12	Wai-San-Ting sand barrier	Clear	2.2	3.5
1999/04/29	Taichung port	Clear	2.0	3.3

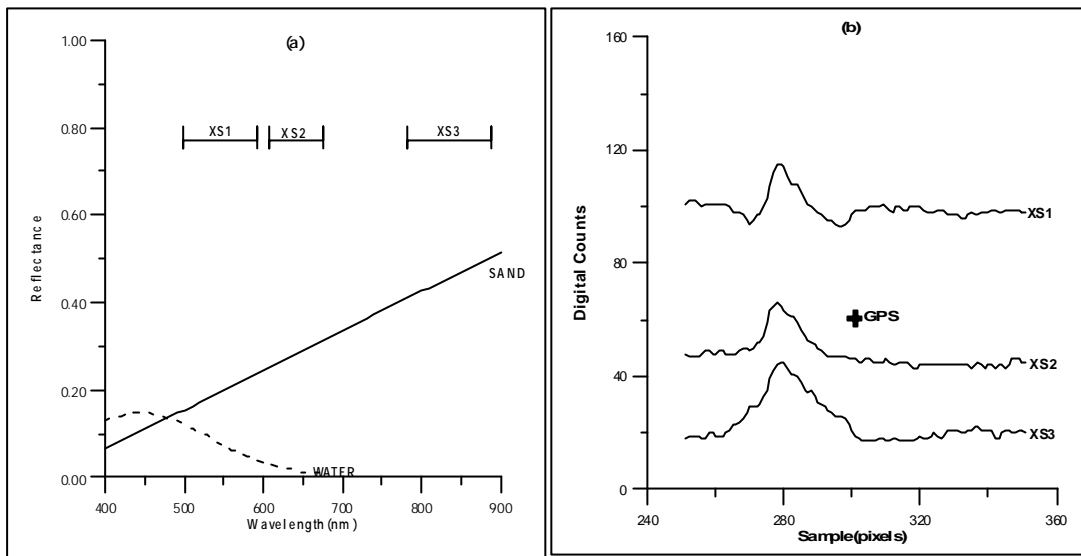


Figure 1. (a)The reflectance of water and sand in 400-900nm. (b) The digital counts of the SPOT HRV bands along the sample direction across the Wai-San-Ting sand barrier, November 12, 1998. on a clear sky condition. The symbol of '+' represents the GPS measurement of the shoreline position.

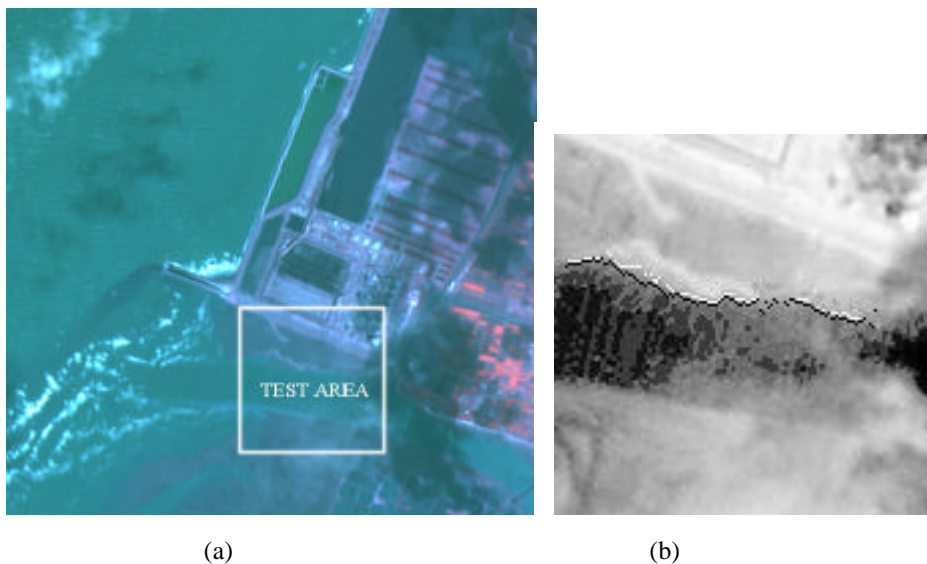


Figure 2. (a)The SPOT HRV image of Taichung port area, January 30, 1996. (b) The shoreline detection by Gradient(black line) and Sobel(white line) operators.

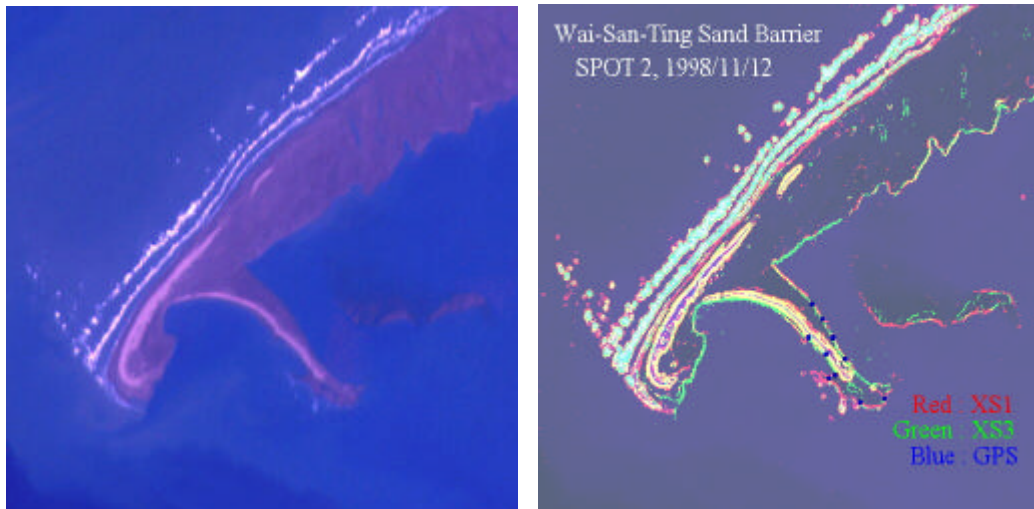


Figure 3. (a) The SPOT HRV image of Wai-San-Ting sand barrier, November 12, 1998. (b) The shoreline detection by Gradient operator from XS1(red) and XS3(green) data. The cyan points mean concurrent GPS measurement of the shoreline position.

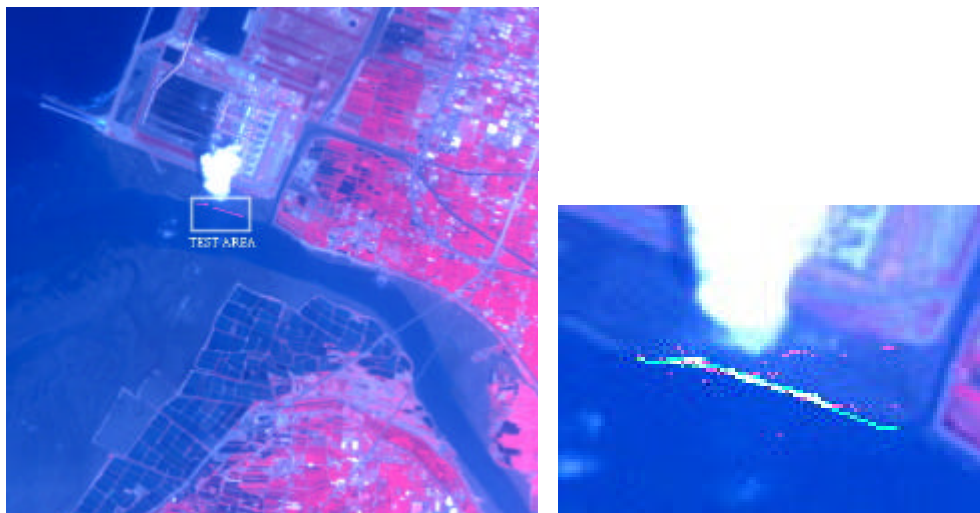


Figure 4. (a) The SPOT HRV image of Taichung port, April 29, 1999. (b) The shoreline detection by the Gradient operator from XS1(red) and XS3(green) data. The white line represents concurrent GPS measurements of the shoreline position.